

Structural Characterization of a Variable-Spin (Porphinato)iron(III) Complex. Molecular Stereochemistry of Bis(3-chloropyridine)(octaethylporphinato)iron(III) Perchlorate at 98 K ($S = 1/2$) and 293 K ($S = 1/2, S = 5/2$)

W. Robert Scheidt,* David K. Geiger, and Kenneth J. Haller

Contribution from the Department of Chemistry, University of Notre Dame, Notre Dame, Indiana 46556. Received September 21, 1981

Abstract: The molecular stereochemistry of the variable-spin (porphinato)iron(III) complex bis(3-chloropyridine)(octaethylporphinato)iron(III) perchlorate has been determined at 98 and 293 K. At 98 K, where the six-coordinate molecule is predominantly in the low-spin state, the average Fe-N_p distance is 1.994 Å and the axial Fe-N distance is 2.031 Å. At 293 K, the magnetic susceptibility is 4.7 μ_B, consistent with a 55:45 thermal mixture of high- and low-spin states. The determination of the "average" structure at 293 K yields an Fe-N_p distance of 2.014 Å and an axial distance of 2.194 Å. These increased distances are consistent with the presence of a substantial fraction of a high-spin state. A crystallographic resolution of spin isomers at 293 K was accomplished. This gives resolved 3-chloropyridine ligand positions which lead to a low-spin axial Fe-N distance of 2.043 Å and a high-spin distance of 2.316 Å. No motion of the iron(III) atom is required in the spin-state transition. Crystal data: (98 K) $a = 10.798$ (4) Å, $b = 11.400$ (3) Å, $c = 9.740$ (3) Å, $\alpha = 113.08$ (2)°, $\beta = 95.66$ (3)°, $\gamma = 72.87$ (3)°, $V = 1053.9$ Å³, $Z = 1$, space group $P\bar{1}$; (293 K) $a = 10.929$ (3) Å, $b = 11.480$ (2) Å, $c = 9.954$ (2) Å, $\alpha = 112.27$ (1)°, $\beta = 94.30$ (2)°, $\gamma = 73.34$ (2)°, $V = 1106.5$ Å³, $Z = 1$, space group $P\bar{1}$.

A number of examples of hemoprotein derivatives possessing an electronic structure in which the iron(III) atom is in thermal equilibrium between the $S = 1/2$ low-spin and the $S = 5/2$ high-spin states have been reported. These hemoprotein species include myoglobin and hemoglobin,¹⁻⁴ cytochrome P-450,^{5,6} and cytochrome *c* peroxidase.⁷ Measurements of the spin interconversion rates in myoglobin derivatives^{8,9} have demonstrated that the rates are extremely fast (rate constants $> 10^7$ s⁻¹). Differences in the temperature-dependent magnetic moments of various hemoprotein species having the same axial ligands demonstrate that the protein matrix can have a significant effect on the spin state equilibrium. However, there is little direct information concerning the stereochemical changes of the heme (i.e., the coordination geometry of the iron(III) atom) upon a change in spin multiplicity for the hemoproteins.

Although a large number of iron(III) complexes that undergo a low-spin high-spin thermal equilibrium are known,¹⁰⁻¹² it was only recently that (porphinato)iron(III) species exhibiting this phenomenon were reported.¹³⁻¹⁵ The observation by Hill, Buchler,

and co-workers¹⁴ that a number of bis(substituted pyridine)(octaethylporphinato)iron(III) complexes display temperature-dependent magnetic moments which could be interpreted in terms of a spin equilibrium between the $S = 1/2$ and $S = 5/2$ states is especially interesting. The bis(3-chloropyridine) complex displays the largest variation in temperature-dependent moments. This complex is reported to show a magnetic moment at 77 K corresponding to an almost pure low-spin state and a moment at room temperature appropriate for an approximately 50:50 mixture of the low- and high-spin states. Gregson has recently reported¹⁶ a quantitative interpretation of the temperature-dependent magnetic properties of these complexes. We have prepared one of these species, bis(3-chloropyridine)(octaethylporphinato)iron(III), as the perchlorate salt, hereinafter written¹⁷ as [Fe(OEP)(3-Clpy)₂](ClO₄). We have determined the molecular stereochemistry of [Fe(OEP)(3-Clpy)₂](ClO₄) at 98 K by single-crystal X-ray diffraction methods; the molecular stereochemistry at this temperature is cleanly interpreted in terms of a low-spin iron(III) porphyrinate complex. We have also examined [Fe(OEP)(3-Clpy)₂](ClO₄) at room temperature (293 K) and have interpreted the diffraction data both in terms of the "average" structure of the molecule¹⁸ and a crystallographic resolution¹⁹ of the structures of the 56:44 mixture of the two spin isomers ($S = 5/2, 1/2$). This latter analysis provides a direct description of the structural changes accompanying the low-spin to high-spin transition in an iron(III) porphyrinate. It is expected that similar coordination group changes will be found in the hemoproteins undergoing this spin-state transition.

Experimental Section

Synthesis of [Fe(OEP)(3-Clpy)₂](ClO₄). In a typical preparation, 200 mg (0.29 mmol) of Fe(OEP)(OCIO₃)₂²⁰ in 35 mL of benzene was treated with 1.0 mL (10.5 mmol) of 3-chloropyridine and allowed to stir for 1 h. A purple precipitate formed and was collected on a medium frit and recrystallized from chloroform and Skellysolve F (180 mg, 0.2 mmol,

- (1) Beetlestone, J.; George, P. *Biochemistry* **1964**, *3*, 707-714.
- (2) Iizuka, T.; Kotani, M. *Biochim. Biophys. Acta* **1968**, *154*, 417-419.
- (b) *Ibid.* **1969**, *181*, 275-286. (c) *Ibid.* **1969**, *194*, 351-363.
- (3) Anusiem, A. C. I.; Kelleher, M. *Biopolymers*, **1978**, *17*, 2047-2055.
- (4) (a) Perutz, M. F.; Sanders, J. K. M.; Chenerv, D. H.; Noble, R. W.; Pennelly, R. R.; Fund, L. W.-M.; Ho, C.; Giannini, I.; Porschke, D.; Winkler, H. *Biochemistry* **1978**, *17*, 3640-3652. (b) Messana, C.; Cerdonio, M.; Shenkin, P.; Noble, R. W.; Fermi, G.; Perutz, R. W.; Perutz, M. F. *Ibid.* **1978**, *17*, 3652-3662.
- (5) Sligar, S. G. *Biochemistry* **1976**, *15*, 5399-5406.
- (6) Lange, R.; Bonfils, C.; Debey, P. *Eur. J. Biochem.* **1977**, *79*, 623-628.
- (7) Yonetani, T.; Iizuka, T.; Asakura, T. *J. Biol. Chem.* **1972**, *247*, 863-868.
- (8) Beattie, J. K.; West, R. J. *J. Am. Chem. Soc.* **1974**, *96*, 1933-1935.
- (9) Dose, E. V.; Tweedle, M. F.; Wilson, L. J.; Sutin, N. *J. Am. Chem. Soc.* **1977**, *99*, 3886-3888.
- (10) For recent reviews, see: (a) Goodwin, H. A. *Coord. Chem. Rev.* **1976**, *18*, 293-325. (b) Martin, R. H.; White, A. H. *Transition Met. Chem. (N.Y.)* **1968**, *4*, 113-198. (c) Barefield, E. K.; Busch, D. H.; Nelson, S. M. *Q. Rev. Chem. Soc.* **1968**, *22*, 457-498.
- (11) Sim, P. G.; Sinn, E.; Petty, R. H.; Merrill, C. L.; Wilson, L. *J. Inorg. Chem.* **1981**, *20*, 1213-1222, and references therein.
- (12) Haddad, M. S.; Lynch, M. W.; Federer, W. D.; Hendrickson, D. N. *Inorg. Chem.* **1981**, *20*, 123-131.
- (13) Kassner, R. J.; Huang, Y.-P. *J. Am. Chem. Soc.* **1979**, *101*, 5807-5810.
- (14) Hill, H. A. O.; Skyte, P. D.; Buchler, J. W.; Lueken, H.; Tonn, M.; Gregson, A. K.; Pellizer, G. *J. Chem. Soc., Chem. Commun.* **1979**, 151-152.
- (15) Collman, J. P.; Sorell, T. N.; Hodgson, K. O.; Kulshrestha, A. K.; Strouse, C. E. *J. Am. Chem. Soc.* **1978**, *99*, 5180-5181.

(16) Gregson, A. K. *Inorg. Chem.* **1981**, *20*, 81-87.

(17) Abbreviations used in this paper: OEP, dianion of octaethylporphyrin; TPP, the dianion of *meso*-tetraphenylporphyrin; Proto IX, the dianion of protoporphyrin IX; 3-Clpy, 3-chloropyridine; py, pyridine; HIm, imidazole; 1-MeIm, 1-methylimidazole; N_p, porphinato nitrogen atom.

(18) Scheidt, W. R.; Geiger, D. K. *J. Chem. Soc., Chem. Commun.* **1979**, 1154-1155.

(19) Katz, B. A.; Strouse, C. E. *J. Am. Chem. Soc.* **1979**, *101*, 6214-6221.

(20) Dolphin, D. H.; Sams, J. R.; Tsin, T. B. *Inorg. Chem.* **1977**, *16*, 711-713.

69%); IR $\nu(\text{ClO}_4)$ 1105, 1090, 628 cm^{-1} ; $\nu(3\text{-Clpy})$ 1570, 1412 cm^{-1} ; $\lambda_{\text{max}}(\text{CHCl}_3)$ 360 (sh), 398, 512, 550 (sh) nm.

Large, well-formed crystals of $[\text{Fe}(\text{OEP})(3\text{-Clpy})_2](\text{ClO}_4)$ were obtained via vapor diffusion of hexane into a 10:1 chloroform/3-chloropyridine solution of $[\text{Fe}(\text{OEP})(3\text{-Clpy})_2](\text{ClO}_4)$. The crystals so obtained were used for magnetic susceptibility studies and the structure determinations.

Synthesis of $[\text{Fe}(\text{TPP})(3\text{-Clpy})_2]\text{ClO}_4$. $[\text{Fe}(\text{TPP})(\text{OClO}_3)]^{21}$ (120 mg (0.14 mmol)) was added to a stirred solution of chloroform (50 mL) and 3-chloropyridine (3.0 mL). After 3 h, the volume was reduced to 25 mL and upon addition of an equal volume of hexane the purple precipitate was collected on a medium frit (110 mg, 0.11 mmol, 79%): IR $\nu(\text{ClO}_4)$ 1107, 1090, 628 cm^{-1} ; $\nu(3\text{-Clpy})$ 1570, 1412 cm^{-1} ; $\lambda_{\text{max}}(\text{CHCl}_3)$ 418, 533 (sh), 573, 635 (sh) nm.

Magnetic Data. Magnetic susceptibilities of crystalline $[\text{Fe}(\text{OEP})(3\text{-Clpy})_2](\text{ClO}_4)$ were measured on a Faraday balance equipped with a Cahn-Ventron R-100 balance and a Varian Fieldial Mark I field-regulated magnet. Field strengths of 7.0, 8.0, and 9.0 kG were employed. The sample was maintained in a nitrogen atmosphere and $\text{Ni}(\text{NH}_4)_2(\text{SO}_4)_2 \cdot 6\text{H}_2\text{O}$ was used as the standard. The following diamagnetic corrections were applied: octaethylporphine, -470×10^{-6} ; 3-chloropyridine, -63×10^{-6} ; and perchlorate, -34×10^{-6} cgs/mol. No field dependence was observed. The average magnetic moments at the given temperature follow: 77 K, 2.7 μ_B ; 100 K, 2.9 μ_B ; 110 K, 3.0 μ_B ; 133 K, 3.1 μ_B ; 170 K, 3.3 μ_B ; 294 K, 4.7 μ_B . The solid state susceptibility data are in agreement with those reported for the hexafluorophosphate salt.¹⁴ Solution susceptibilities were determined in methylene chloride (9.8 mg/mL) by the Evans method²² on a Varian XL-100 Fourier transform NMR spectrometer. The magnetic moments found are as follows: 173 K, 3.6 μ_B ; 193 K, 3.8 μ_B ; 203 K, 3.9 μ_B ; 213 K, 4.1 μ_B ; 223 K, 4.1 μ_B ; 233 K, 4.3 μ_B ; 248 K, 4.3 μ_B ; 263 K, 4.3 μ_B ; 273 K, 4.5 μ_B ; 303 K, 4.5 μ_B ; 313 K, 4.6 μ_B . In chloroform solution at 313 K, $\mu_{\text{eff}} = 4.5 \mu_B$, in agreement within experimental error of the previously reported value.^{14,23} However, the tetraphenylporphine analogue is near the low-spin value at room temperature (solid state) with $\mu_{\text{eff}} = 2.7 \mu_B$. (The diamagnetic correction used²⁴ for tetraphenylporphine was -700×10^{-6} cgs/mol).

Preliminary X-ray Examination and Data Collection. A single crystal with approximate dimensions of $0.4 \times 0.4 \times 0.6$ mm was used in all experiments. Preliminary examination on a Nicolet P1 diffractometer established a one-molecule triclinic unit cell, space group $P1$ or $P\bar{1}$. Measurements were made at ambient laboratory temperature (293 ± 1 K) and at low temperature (98 ± 5 K) with a Nicolet LT-1 attachment for the diffractometer. Least-squares refinement of the setting angles of automatically centered reflections led to the cell constants reported in Table I. Intensity data were collected at the two temperatures, and details of the intensity collection parameters are summarized in Table I. For the low-temperature data set, the crystalline sample was lost after all intensities to $2\theta \leq 54.9^\circ$ had been measured and forced termination of data collection. Intensity data were reduced as previously described.²⁵

Structure Solution and Refinements. The structure was initially solved by using the 293 K data set with heavy-atom techniques.²⁶ The choice of the space group $P1$ was confirmed by all subsequent developments during the structure solution and refinement. The space group $P\bar{1}$ with the one-molecule unit cell leads to the requirement that the $[\text{Fe}(\text{OEP})(3\text{-Clpy})_2]^+$ moiety has a crystallographically imposed center of symmetry at the iron(III) atom. The Patterson map could be interpreted to yield the coordinates of the chlorine atom of the ligand and most of the atoms of the unique half of the porphinato core. Subsequent cycles of difference Fourier syntheses yielded the remainder of the atoms of the porphinato ligand and the axial pyridine. The perchlorate ion was found to be disordered around the inversion center at $1/2, 1/2, 0$. This disorder was satisfactorily modeled with an entire ClO_4^- group, with atomic occupancies of 0.5, slightly displaced (~ 0.3 Å) from the inversion center. After several cycles of isotropic block-diagonal least-squares refinement, a difference Fourier synthesis gave peaks convincingly located for all

Table I. Summary of Crystal Data and Intensity Collection Parameters for $[\text{Fe}(\text{OEP})(3\text{-Clpy})_2] \cdot \text{ClO}_4$

formula	$\text{FeCl}_3\text{O}_4\text{N}_6\text{C}_{46}\text{H}_{52}$	$\text{FeCl}_3\text{O}_4\text{N}_6\text{C}_{46}\text{H}_{52}$
formula wt, amu	915.2	915.2
space group	$P\bar{1}$	$P\bar{1}$
T , K	293	98
a , Å	10.929 (3)	10.798 (4)
b , Å	11.480 (2)	11.400 (3)
c , Å	9.954 (2)	9.740 (3)
α , deg	112.27 (1)	113.08 (2)
β , deg	94.30 (2)	95.66 (3)
γ , deg	73.34 (2)	72.87 (3)
V , Å ³	1106.5	1053.9
Z	1	1
density (calcd), g/cm ³	1.373	1.442
density (obsd), g/cm ³	1.39	
radiation	graphite monochromated Mo $K\alpha$ ($\lambda = 0.71073$ Å)	
scan technique	θ - 2θ	θ - 2θ
scan range	0.6° below $K\alpha_1$ to 0.6° above $K\alpha_2$	
scan rate, deg/min	2-24	2-24
background	0.5 times scan time at extremes of scan	profile analysis
2θ limits	3.5-58.7	3.5-54.9
criterion for observation	$F_o > 3\sigma(F_o)$	$F_o > 3\sigma(F_o)$
unique obsd data	5228	5315
μ , mm ⁻¹	0.519	0.543
R_1	0.045	0.043
R_2	0.063	0.062
goodness of fit	1.948	2.279

hydrogen atoms of the molecule. Hydrogen atom positions from this Fourier synthesis were included in subsequent least-squares refinement cycles; both the coordinates and an isotropic temperature factor for all hydrogen atom parameters were exceptionally well-behaved in the least-squares refinement. Least-squares refinement was carried to convergence for the 399 parameters which included anisotropic temperature factors for all heavy atoms of the structure (the parameter count includes the refined hydrogen atom parameters). At convergence, the final values for the discrepancy indices²⁷ were $R_1 = 0.045$ and $R_2 = 0.063$, with a final data/parameter ratio of 13.1. The highest peak in the final difference Fourier map was $0.44 \text{ e}/\text{Å}^3$, and most peaks were much less than this value. Final atomic positional parameters are listed in Table II (supplementary material). Table II also lists the equivalent isotropic temperature factors for atoms refined anisotropically. Table III (supplementary material) gives a final listing of the anisotropic temperature factors. The corresponding data derived from the refinement of structure at 98 K is given as the second entry in both Tables II and III. Final listings of the observed and calculated structure amplitudes ($\times 10$) are available as supplementary material.

The structure of the molecule at 98 K was obtained by using the previously determined coordinates of the core to establish phases; the resulting difference Fourier synthesis established the coordinates of the axial ligand. Refinement was carried out as before. At convergence, $R_1 = 0.043$ and $R_2 = 0.062$. A final difference Fourier had its largest two peaks of $0.6 \text{ e}/\text{Å}^3$ near the iron atom; all other peaks were $< 0.5 \text{ e}/\text{Å}^3$. Final parameters are reported in Tables II and III and a listing of structure amplitudes is available as supplementary material. A table of refined hydrogen atom positions is given in the supplementary material.

The systematic differences between the structure of $[\text{Fe}(\text{OEP})(3\text{-Clpy})_2](\text{ClO}_4)$ at the two temperatures were consistent with the hypothesis that the room temperature structure represented the "average" structure of the high-spin and low-spin isomers of the molecule. A crystallographic resolution of the high-spin and low-spin forms of $[\text{Fe}(\text{OEP})(3\text{-Clpy})_2](\text{ClO}_4)$ at 293 K was then carried out by using full-matrix rigid-group refinement techniques. The rigid-group description of the 3-chloropyridine ligand was obtained from the 98 K structure. The initial crystallographic model consisted of a single porphinato core, the perchlorate anion, and two rigid-group axial ligands with initial atomic occupancies of 0.5 and separated along the Fe-N_{ax} vector so that $\text{Fe-N}(\text{LS}) = 2.03$ Å and $\text{Fe-N}(\text{HS}) = 2.35$ Å. Resolution of the two positions of the porphinato core atoms was not attempted since the expected sep-

(21) Mashiko, T.; Kastner, M. E.; Spartalian, K.; Scheidt, W. R.; Reed, C. A. *J. Am. Chem. Soc.* **1978**, *100*, 6354-6362.

(22) Evans, D. F. *J. Chem. Soc.* **1959**, 2003-2005.

(23) Skyte, P. D. D. Phil. Thesis, University of Oxford, 1977.

(24) Eaton, S. S.; Eaton, G. R. *Inorg. Chem.* **1980**, *19*, 1095-1096.

(25) Scheidt, W. R. *J. Am. Chem. Soc.* **1974**, *96*, 84-89.

(26) Programs used in this study included local modifications of Jacobson's ALFF and ALLS, Busing and Levy's ORFFE and ORFLS, and Johnson's ORTEP. Atomic form factors were from Cromer and Mann [Cromer, D. T.; Mann, J. B. *Acta Crystallogr., Sect. A* **1968**, *24*, 321-323], with real and imaginary corrections for anomalous dispersion in the form factor of the iron and chlorine atoms from Cromer and Liberman [Cromer, D. T.; Liberman, D. J. *J. Chem. Phys.* **1970**, *53*, 1891-1898]. Scattering factors for hydrogen were from Stewart et al. [Stewart, R. F.; Davidson, E. R.; Simpson, W. T. *Ibid.* **1965**, *42*, 3175-3187].

(27) $R_1 = \sum |F_o| - |F_c| / \sum |F_o|$ and $R_2 = [\sum w(|F_o| - |F_c|)^2 / \sum w(F_o)^2]^{1/2}$

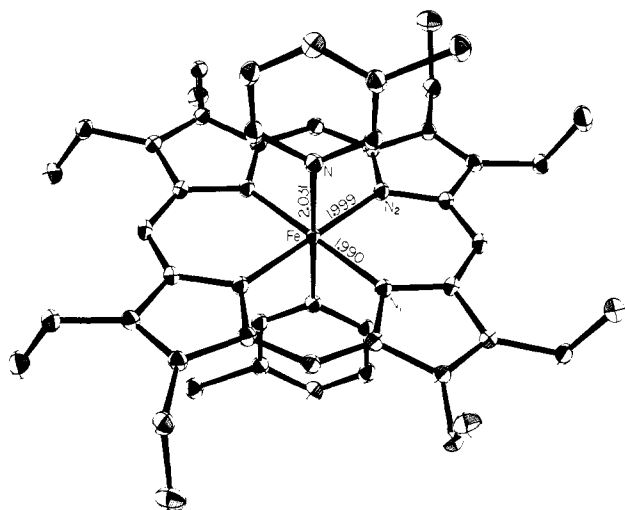


Figure 1. A computer-drawn model in perspective of the $[\text{Fe}(\text{OEP})(3\text{-Clpy})_2](\text{ClO}_4)$ molecule at 98 K. The labeling scheme for the crystallographically unique atoms is given. Bond distances in the coordination group are shown. Ellipsoids are contoured to enclose 50% of the electron density.

Table V. Bond Distances in $[\text{Fe}(\text{OEP})(3\text{-Clpy})_2](\text{ClO}_4)^a$

type	distance, Å	type	distance, Å	type	distance, Å
$\text{Fe}-\text{N}_1^b$	2.011 (1)	$\text{C}_{a3}-\text{C}_{b3}$	1.445 (2)	$\text{C}_{41}-\text{C}_{42}$	1.526 (3)
	1.990 (2)		1.447 (2)		1.531 (2)
$\text{Fe}-\text{N}_2$	2.017 (1)	$\text{C}_{a4}-\text{C}_{m1}$	1.384 (2)	N_3-C_1	1.342 (2)
	1.999 (2)		1.388 (2)	N_3-C_5	1.349 (2)
$\text{Fe}-\text{N}_3$	2.194 (2)	$\text{C}_{a4}-\text{C}_{b4}$	1.447 (2)	N_3-C_5	1.346 (2)
	2.031 (2)		1.447 (2)		1.348 (2)
N_1-C_{a1}	1.381 (2)	$\text{C}_{b1}-\text{C}_{11}$	1.507 (2)	C_1-C_2	1.380 (3)
	1.383 (2)		1.499 (2)		1.385 (2)
N_1-C_{a2}	1.381 (2)	$\text{C}_{b2}-\text{C}_{21}$	1.502 (2)	C_2-C_3	1.385 (3)
	1.384 (2)		1.503 (2)		1.391 (2)
N_2-C_{a3}	1.378 (2)	$\text{C}_{b3}-\text{C}_{31}$	1.505 (2)	C_3-C_4	1.383 (3)
	1.378 (2)		1.502 (2)		1.387 (2)
N_2-C_{a4}	1.382 (2)	$\text{C}_{b4}-\text{C}_{41}$	1.506 (2)	C_4-C_5	1.380 (3)
	1.376 (2)		1.500 (2)		1.382 (2)
$\text{C}_{a1}-\text{C}_{m1}$	1.380 (2)	$\text{C}_{b1}-\text{C}_{b2}$	1.360 (2)	C_4-Cl	1.730 (2)
	1.380 (2)		1.365 (2)		1.727 (2)
$\text{C}_{a1}-\text{C}_{b1}$	1.447 (2)	$\text{C}_{b3}-\text{C}_{b4}$	1.361 (2)	Cl_1-O_1	1.436 (4)
	1.447 (2)		1.371 (2)		1.445 (3)
$\text{C}_{a2}-\text{C}_{m2}$	1.381 (2)	$\text{C}_{11}-\text{C}_{12}$	1.503 (3)	Cl_1-O_2	1.401 (5)
	1.383 (2)		1.530 (2)		1.424 (3)
$\text{C}_{a2}-\text{C}_{b2}$	1.446 (2)	$\text{C}_{21}-\text{C}_{22}$	1.513 (3)	Cl_1-O_3	1.444 (6)
	1.446 (2)		1.526 (2)		1.435 (4)
$\text{C}_{a3}-\text{C}_{m3}$	1.386 (2)	$\text{C}_{31}-\text{C}_{32}$	1.526 (3)	Cl_1-O_4	1.293 (5)
	1.384 (2)		1.533 (2)		1.422 (3)

^a The numbers in parentheses are the estimated standard deviations. ^b For each distance, the first line gives atomic distances at 293 K; the second line, from data collected at 98 K.

ation in coordinated between the spin isomers is $< \sim 0.05$ Å. Refinement cycles utilized anisotropic temperature factors for all atoms except those of the rigid groups which were assigned individual isotropic temperature factors. Toward the end of the refinement, the rigid-group constraints were slightly relaxed, with the chlorine atom of each group allowed independent coordinates and anisotropic temperature factors. Occupancy factors of the chlorine atoms were constrained to the same value as their respective rigid group. The two rigid-group occupancies were constrained to sum to unity. At convergence, the occupancy factors for the high- and low-spin ligands were 0.56 and 0.44, respectively. Final values of the discrepancy indices were $R_1 = 0.0471$ and $R_2 = 0.0636$. For comparison, a refinement with a single rigid group and an independent anisotropic chlorine atom ($\text{Fe}-\text{N} = 2.193$ Å) gave $R_1 = 0.0543$ and $R_2 = 0.0746$. Except for a few hydrogen atom positions, no positional parameter of the porphyrin ligand in the two rigid-group refinement changed by more than 1σ from the corresponding value in the completely unconstrained refinement. Table IV (supplementary material) presents the derived coordinates of the two pyridine ligands of the spin isomers. A listing of the observed and calculated structure amplitudes ($\times 10$) is

Table VI. Bond Angles in $[\text{Fe}(\text{OEP})(3\text{-Clpy})_2](\text{ClO}_4)^a$

type	angle, deg	type	angle, deg
$\text{N}_1-\text{Fe}-\text{N}_2^b$	89.54 (5)	$\text{C}_{a4}-\text{C}_{b4}-\text{C}_{b3}$	106.92 (14)
	89.49 (6)		106.59 (13)
$\text{N}_1-\text{Fe}-\text{N}_3$	90.11 (5)	$\text{C}_{a4}-\text{C}_{b4}-\text{C}_{41}$	124.13 (15)
	90.07 (5)		124.66 (13)
$\text{N}_2-\text{Fe}-\text{N}_3$	90.97 (6)	$\text{C}_{b3}-\text{C}_{b4}-\text{C}_{41}$	128.93 (15)
	90.69 (6)		128.71 (14)
$\text{C}_{a1}-\text{N}_1-\text{C}_{a2}$	105.67 (12)	$\text{C}_{b1}-\text{C}_{11}-\text{C}_{12}$	113.31 (16)
	105.06 (12)		113.77 (13)
$\text{C}_{a3}-\text{N}_2-\text{C}_{a4}$	105.80 (12)	$\text{C}_{b2}-\text{C}_{21}-\text{C}_{22}$	113.34 (15)
	105.09 (12)		113.72 (13)
$\text{N}_1-\text{C}_{a1}-\text{C}_{b1}$	110.09 (14)	$\text{C}_{b3}-\text{C}_{31}-\text{C}_{32}$	112.52 (16)
	110.58 (13)		112.23 (13)
$\text{N}_1-\text{C}_{a1}-\text{C}_{m1}$	124.80 (14)	$\text{C}_{b4}-\text{C}_{41}-\text{C}_{42}$	113.12 (16)
	124.85 (14)		113.52 (14)
$\text{C}_{b1}-\text{C}_{a1}-\text{C}_{m1}$	125.09 (15)	$\text{C}_1-\text{N}_3-\text{C}_5$	117.65 (16)
	124.53 (14)		118.01 (14)
$\text{N}_1-\text{C}_{a2}-\text{C}_{b2}$	110.43 (14)	$\text{N}_3-\text{C}_1-\text{C}_2$	123.22 (17)
	110.95 (13)		122.93 (14)
$\text{N}_1-\text{C}_{a2}-\text{C}_{m2}$	124.63 (14)	$\text{C}_1-\text{C}_2-\text{C}_3$	119.31 (17)
	125.13 (14)		119.38 (15)
$\text{C}_{b2}-\text{C}_{a2}-\text{C}_{m2}$	124.92 (15)	$\text{C}_3-\text{C}_4-\text{Cl}$	119.59 (16)
	123.91 (14)		119.58 (13)
$\text{N}_2-\text{C}_{a3}-\text{C}_{b3}$	110.34 (14)	$\text{C}_5-\text{C}_4-\text{Cl}$	119.74 (14)
	111.22 (13)		119.39 (12)
$\text{N}_2-\text{C}_{a3}-\text{C}_{m2}'$	124.69 (14)	$\text{C}_2-\text{C}_3-\text{C}_4$	117.36 (19)
	125.42 (14)		117.19 (15)
$\text{C}_{b3}-\text{C}_{a3}-\text{C}_{m2}'$	124.97 (15)	$\text{C}_3-\text{C}_4-\text{C}_5$	120.63 (18)
	123.36 (14)		120.99 (15)
$\text{N}_2-\text{C}_{a4}-\text{C}_{b4}$	110.06 (14)	$\text{C}_4-\text{C}_5-\text{N}_3$	121.82 (16)
	110.96 (13)		121.49 (14)
$\text{N}_2-\text{C}_{a4}-\text{C}_{m1}$	124.49 (14)	$\text{Fe}-\text{N}_1-\text{C}_{a1}$	127.41 (11)
	124.46 (14)		127.77 (10)
$\text{C}_{b4}-\text{C}_{a4}-\text{C}_{m1}$	125.43 (14)	$\text{Fe}-\text{N}_1-\text{C}_{a2}$	126.77 (10)
	124.56 (14)		126.97 (10)
$\text{C}_{a1}-\text{C}_{m1}-\text{C}_{a4}$	126.19 (15)	$\text{Fe}-\text{N}_2-\text{C}_{a3}$	126.60 (10)
	125.22 (14)		126.72 (10)
$\text{C}_{a2}-\text{C}_{m2}-\text{C}_{a3}'$	126.75 (15)	$\text{Fe}-\text{N}_2-\text{C}_{a4}$	127.41 (10)
	125.09 (14)		128.01 (10)
$\text{C}_{a1}-\text{C}_{b1}-\text{C}_{b2}$	107.16 (14)	$\text{Fe}-\text{N}_3-\text{C}_1$	120.99 (12)
	107.00 (13)		120.88 (11)
$\text{C}_{a1}-\text{C}_{b1}-\text{C}_{11}$	124.55 (15)	$\text{Fe}-\text{N}_3-\text{C}_5$	121.33 (12)
	124.87 (14)		121.08 (11)
$\text{C}_{b2}-\text{C}_{b1}-\text{C}_{11}$	128.26 (15)	$\text{O}_1-\text{Cl}_2-\text{O}_2$	102.21 (35)
	128.05 (14)		108.67 (19)
$\text{C}_{a2}-\text{C}_{b2}-\text{C}_{b1}$	106.63 (14)	$\text{O}_1-\text{Cl}_1-\text{O}_3$	103.72 (35)
	106.39 (13)		108.70 (19)
$\text{C}_{a2}-\text{C}_{b2}-\text{C}_{21}$	124.59 (15)	$\text{O}_1-\text{Cl}_1-\text{O}_4$	103.42 (46)
	124.74 (14)		108.85 (19)
$\text{C}_{b1}-\text{C}_{b2}-\text{C}_{21}$	128.77 (15)	$\text{O}_2-\text{Cl}_1-\text{O}_3$	111.47 (50)
	128.85 (14)		108.42 (26)
$\text{C}_{a3}-\text{C}_{b3}-\text{C}_{b4}$	106.88 (14)	$\text{O}_2-\text{Cl}_1-\text{O}_4$	121.56 (57)
	106.14 (13)		112.21 (22)
$\text{C}_{a3}-\text{C}_{b3}-\text{C}_{31}$	124.36 (15)	$\text{O}_3-\text{Cl}_1-\text{O}_4$	111.93 (64)
	124.83 (14)		109.92 (26)
$\text{C}_{b4}-\text{C}_{b3}-\text{C}_{31}$	128.75 (15)		
	129.03 (14)		

^a The numbers in parentheses are the estimated standard deviations. ^b For each angle, the first line gives angles from data collected at 293 K; the second line, from data collected at 98 K.

available as supplementary material.

Results and Discussion

Structure at 98 K. The structure of $[\text{Fe}(\text{OEP})(3\text{-Clpy})_2](\text{ClO}_4)$ at 98 K is shown in Figure 1. The molecule has a crystallographically imposed center of symmetry at the iron(III) atom. Individual values of bond distances and angles for the crystallographically unique portion of the molecule are given in Table V and VI, respectively. Figure 2 presents a formal diagram of a porphyrin core displaying the perpendicular displacements, in units of 0.01 Å, of each unique atom from the mean plane of the 24-atom core. The deviation from exact planarity is unremarkable. Figure 2 also presents the average values for the chemically distinct bond distances and angles. The numbers in parentheses for these averages and other averaged values are the estimated standard

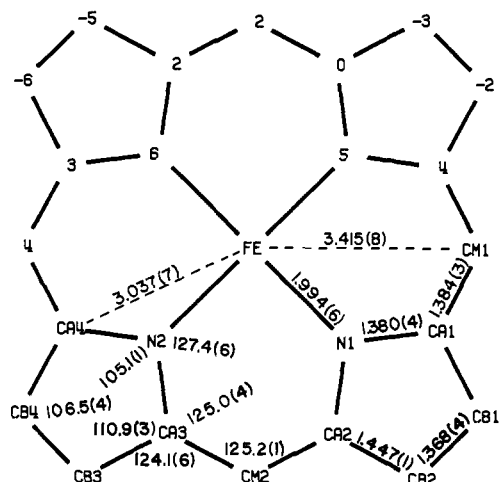


Figure 2. A formal diagram of a porphinato core displaying, for the molecule at 98 K, the average values of the bond parameters. Also displayed are the perpendicular displacements, in units of 0.01 Å, of each crystallographically unique atom of the core from the mean plane of the 24-atom core. Displacements of the centrosymmetrically related atoms are equal in magnitude and opposite in sign.

deviations calculated on the assumption that the values are drawn from the same population.

The molecular parameters of $[\text{Fe}(\text{OEP})(3\text{-Clpy})_2](\text{ClO}_4)$ are clearly consistent with those expected²⁸ for a low-spin six-coordinate (porphinato)iron(III) complex. The average Fe–N_p distance (N_p is a porphinato nitrogen atom) is 1.994 (6) Å, well within the range (1.970 (14)–2.000 (6) Å) observed^{29–34} for other low-spin (porphinato)iron(III) complexes.³⁵ The axial Fe–N distance is 2.031 (2) Å, again well within the range of previously observed values for low-spin species. The Fe–N(py) distance in $[\text{Fe}(\text{TPP})(\text{CN})(\text{py})]^{33}$ is 2.075 (3) Å and in $[\text{Fe}(\text{TPP})(\text{N}_3)(\text{py})]^{31}$ is 2.089 (6) Å. Fe–N(imidazole) distances are slightly shorter, 1.974 (24) Å in $[\text{Fe}(\text{TPPe})(\text{HIm})_2]\text{Cl}^{29}$ and 1.977 (16) Å in $[\text{Fe}(\text{Proto IX})(1\text{-MeIm})_2]^{30}$. The dihedral angle between the pyridine ligand plane and the mean plane of the 24-atom core is 88.6°. The orientation of the 3-chloropyridine ligand with respect to the porphinato core is quite favorable; the angle between the 3-chloropyridine plane and the coordinate plane containing Fe, N₁, and N₃ is 41°. This angle, frequently denoted as ϕ , leads to minimum nonbonded interaction between the porphinato core atoms and axial ligand hydrogen atoms at a value of 45°.

In summary, the structural features for $[\text{Fe}(\text{OEP})(3\text{-Clpy})_2](\text{ClO}_4)$ at 98 K are quite in accord with those expected for a low-spin ($S = 1/2$) species. All other features of the structure are normal. There are no unusual nonbonded intermolecular distances. Despite the disorder in the perchlorate anion, the ion is crystallographically well-behaved. The O–Cl–O angles range from 108.4 (3) to 112.2 (2)°; the Cl–O distances range from 1.422 (3) to 1.445 (3) Å.

Structure at 298 K: The Average Structure. The temperature-dependent magnetic moments of $[\text{Fe}(\text{OEP})(3\text{-Clpy})_2](\text{ClO}_4)$ have been interpreted^{14,16,23} in terms of an $S = 1/2$ to $S = 5/2$ spin

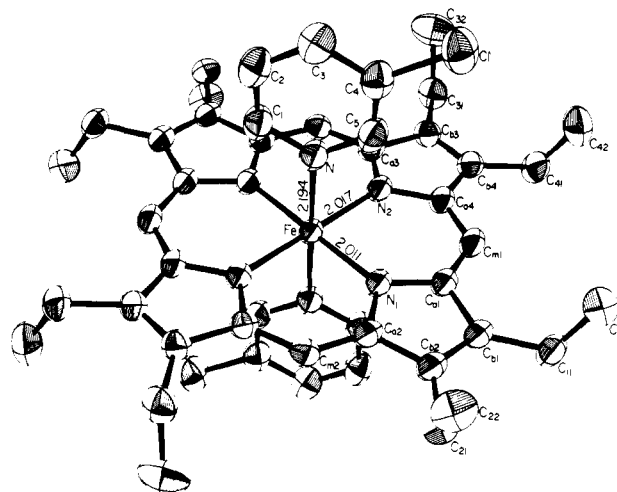


Figure 3. A computer-drawn model displaying the structure of $[\text{Fe}(\text{OEP})(3\text{-Clpy})_2](\text{ClO}_4)$ at 293 K. The same information presented in Figure 1 is given here.

equilibrium. The diffraction data collected for $[\text{Fe}(\text{OEP})(3\text{-Clpy})_2](\text{ClO}_4)$ at 293 K were initially interpreted in terms of the "average" structure of the thermal mixture of the two spin states. The structural results obtained are displayed in Figure 3. Comparison of Figure 3 with Figure 1 makes evident that there are significant differences in the geometry of the coordination groups at the two temperatures. These differences are consistent with the presence of a significant amount of a high-spin species at 293 K and with the fact that the determination of structure is that of the average structure of two spin states of the molecule. The axial Fe–N distance of 2.194 Å is substantially longer than that expected for a pure low-spin species. The average equatorial Fe–N_p distance of 2.014 (4) Å is about midway between the 1.990-Å value appropriate for low-spin six-coordinate (porphinato)iron(III) complexes and the 2.045-Å value observed for two high-spin six-coordinate complexes, a bis(aquo)³⁶ and a bis(tetramethylene sulfoxide)(*meso*-tetraphenylporphinato)iron(III) complex.³⁷ There thus appears to be some porphinato core expansion, consistent with a high-spin state, in $[\text{Fe}(\text{OEP})(3\text{-Clpy})_2](\text{ClO}_4)$ at 293 K. Indeed, an interpolation of the observed equatorial distance, assuming that it is linearly dependent on the relative fractions of low- and high-spin states, leads to a calculated value of 44% high spin. This crystallographic value is in good agreement with a value of ~55% calculated from the magnetic susceptibility.³⁸ It may also be noted that the changes in cell constants, with temperature, are consistent with larger changes in the molecular axial direction than in the equatorial direction; the change is about 2.5 times larger in the axial direction.

Figure 4 is an ORTEP plot that shows the relative shifts in the pyridine ligand position at the two temperatures. The figure also displays the qualitative differences in the temperature factors in the structures at the two temperatures. The inner ellipsoids, contoured to enclose 50% of the associated electron density, represent the results derived from the 98 K data; the outer ellipsoids, on the same scale, are those derived from the 293 K data. All atom pairs, except those of the pyridine ligand, are referred to common centers. It can also be seen in Figure 4 that the orientation of the pyridine ligand, with respect to the porphinato core, is effectively the same at both temperatures. Table VII presents the mean B_{11} values for selected groups of atoms and the ratio of their values at the two temperatures. It can be seen that the pyridine atom ratio is larger than those of the various porphinato atoms but is comparable to those of the perchlorate group atoms.

(28) Scheidt, W. R.; Reed, C. A. *Chem. Rev.* **1981**, *81*, 543.

(29) Collins, D. M.; Countryman, R.; Hoard, J. L. *J. Am. Chem. Soc.* **1972**, *94*, 2066–2072.

(30) Little, R. G.; Dymock, K. R.; Ibers, J. A. *J. Am. Chem. Soc.* **1975**, *97*, 4532–4539.

(31) Adams, K. M.; Rasmussen, P. G.; Scheidt, W. R.; Hatano, K. *Inorg. Chem.* **1979**, *18*, 1892–1899.

(32) Kirner, J. F.; Hoard, J. L.; Reed, C. A. "Abstracts of Papers", 175th National Meeting of the American Chemical Society, Anaheim, CA, March 1978; American Chemical Society: Washington, D.C., 1978; INOR 14.

(33) Scheidt, W. R.; Haller, K. J.; Lee, Y. J.; Luangdilok, W.; Anzai, K.; Hatano, K., to be published.

(34) Scheidt, W. R.; Haller, K. J.; Hatano, K. *J. Am. Chem. Soc.* **1980**, *102*, 3017–3021.

(35) A slightly longer Fe–N_p distance (2.008 (7) Å) is observed for bis(benzenethiolato)(tetraphenylporphinato)iron(III) at 115 K: Byrn, M. P.; Strouse, C. E. *J. Am. Chem. Soc.* **1981**, *103*, 2633–2635.

(36) Scheidt, W. R.; Cohen, I. A.; Kastner, M. E. *Biochemistry* **1978**, *18*, 3546–3552.

(37) Mashiko, T.; Kastner, M. E.; Spartalian, K.; Scheidt, W. R.; Reed, C. A. *J. Am. Chem. Soc.* **1978**, *100*, 6354–6362.

(38) The fraction, α , in the high-spin state is calculated by $(\mu_{\text{eff}})^2 = \alpha(\mu_{\text{HS}})^2 + (1 - \alpha)(\mu_{\text{LS}})^2$, where $\mu_{\text{HS}} = 5.9$ and μ_{LS} was taken to be 2.4.

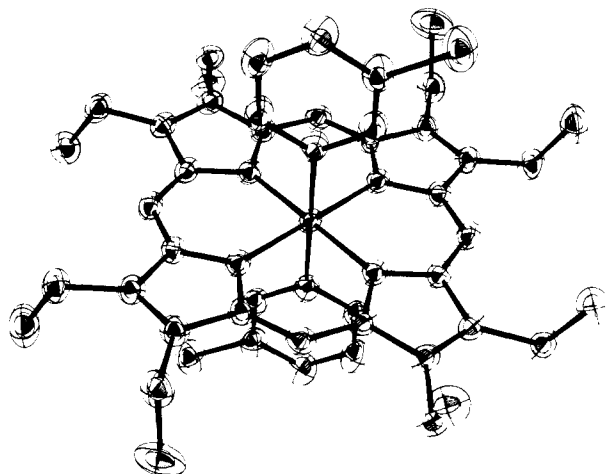


Figure 4. A computer-drawn model of $[\text{Fe}(\text{OEP})(3\text{-Clpy})_2](\text{ClO}_4)$ showing the relative shifts in the 3-chloropyridine ligand position at 98 and 293 K. The inner ellipsoids represent the apparent thermal motion at 98 K, the outer ellipsoids that at 293 K. Both are contoured at the 50% probability level. For clarity, all atom pairs except those of the 3-chloropyridine ligand are referred to common centers.

Table VII. Average B_{ij} Values at 293 and 98 K (\AA^2)

	293 K	98 K	293 K/ 98 K
Fe	2.71	0.97	2.79
porphinato core	3.10	1.26	2.46
methyl carbons	5.74	2.04	2.81
3-chloropyridine ligand	3.96	1.36	2.91
perchlorate	10.53	3.51	3.00

Structure at 298 K: The Resolved Structure. An attempt to crystallographically resolve the structure of the spin isomers led to two axial ligand positions at 2.043 and 2.316 \AA from the iron(III) atom. These positions are associated with the low-spin and high-spin forms of the molecule. Resolution of the small but expected real differences in the porphinato core atoms was not attempted. The results of the crystallographic resolution of the two spin states, at 293 K, are shown in Figure 5. The two pyridine ring planes are slightly (4.6°) twisted with respect to each other. The average distance between corresponding pairs of atoms in the two groups is 0.30 \AA .

The success of the crystallographic resolution of the spin isomers of $[\text{Fe}(\text{OEP})(3\text{-Clpy})_2](\text{ClO}_4)$ is evidenced by (a) the close agreement in the low-spin distance (2.043 \AA) with the value from the unambiguously low-spin form of the molecule (2.031 \AA), (b) the agreement of the occupancy-weighted average Fe–N distance (2.196 \AA) with the 2.194- \AA value obtained from the average structure, and (c) the agreement of the occupancy of the high-spin form (56%) determined from the refinement with the value estimated directly from the magnetic moment (55%).

Comparison of the Structures of the Two Spin States. The total structural change for $[\text{Fe}(\text{OEP})(3\text{-Clpy})_2](\text{ClO}_4)$ in the two spin states can be described as an 0.27- \AA increase in the axial Fe–N bonds and porphinato core expansion leading to a probable increase of ~ 0.055 \AA in the equatorial Fe–N_p bonds in the high-spin state. These bond-length increases are the result of singly populating the $d_{x^2-y^2}$ and d_{z^2} orbitals. The anisotropic increase in bond lengths is, of course, the result of the quasi-rigid porphinato macrocycle which resists exceptional radial expansion. Similar magnitudes of bond elongation are observed in other metalloporphyrin complexes when these critical orbitals are populated. Thus in the isoelectronic d^4 complexes, $[\text{Mn}(\text{TPP})(\text{py})(\text{Cl})]$ (high spin)³⁹ and $[\text{Cr}(\text{TPP})(\text{py})_2]$ (low spin),⁴⁰ the axial bond length change is 0.28 \AA on populating d_{z^2} . An increase of ~ 0.08 \AA in the equatorial Ni–N_p bonds is observed in a high-spin six-coordinate nickel(II)

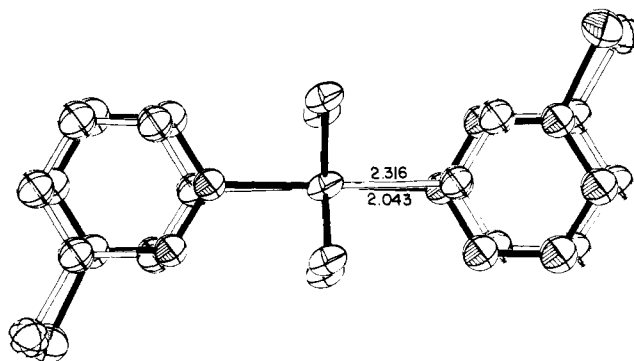


Figure 5. A diagram showing the results of the crystallographic resolution of the 3-chloropyridine ligand at 293 K. The ellipsoids drawn with full lines are those of the low-spin form and ellipsoids drawn with dotted lines represent the high-spin position of the ligand. All are drawn at the 50% level.

porphyrinate relative to the low-spin four-coordinate species⁴¹ as a result of populating the $d_{x^2-y^2}$ orbital.

The average increase in an iron–ligand bond in $[\text{Fe}(\text{OEP})(3\text{-Clpy})_2](\text{ClO}_4)$ is 0.13 \AA . This increase is notably similar to the average increase for other six-coordinate d^5 Fe(III) complexes undergoing this spin-state change. Bond length changes of this magnitude are found in tridentate N_4O_2 complexes,¹¹ hexadentate N_4O_2 complexes,⁴² and bidentate dithiocarbamate complexes.^{43–45}

Conclusions.

The obligatory structural changes that accompany the low-spin to high-spin transition in $[\text{Fe}(\text{OEP})(3\text{-Clpy})_2](\text{ClO}_4)$ are (a) a substantial elongation (0.27 \AA) of the axial Fe–N bonds, and (b) an expansion (~ 0.055 \AA) of the porphinato core. The average increase in the iron–ligand bond distance is 0.13 \AA . Movement of the iron(III) atom with respect to the porphinato plane is *not* required. It is expected that similar molecular motions of the porphinato and axial ligands and minimal motion of the iron(III) atom can be found in hemoproteins undergoing this spin-state transition.⁴⁶ The relative ease of the required molecular motions accompanying the spin-state transition may be influenced by protein structure and thus explain quantitative differences in magnetic behavior of hemoproteins having identical axial ligands for the heme.

Acknowledgment. We thank the National Institutes of Health for support of this work under Grant HL-15627. The support of the Research Corporation for the purchase of the low-temperature apparatus is gratefully acknowledged. We also thank Dr. H. A. O. Hill for providing us with a copy of P. D. Skyte's thesis. We are grateful to Professors P. G. Rasmussen and Larry Garber for access to magnetic susceptibility apparatus.

Registry No. $[\text{Fe}(\text{OEP})(3\text{-Clpy})_2]\text{ClO}_4$, 71414-31-8; $\text{Fe}(\text{OEP})(\text{OCIO}_3)$, 50540-30-2; $[\text{Fe}(\text{TPP})(3\text{-Clpy})_2]\text{ClO}_4$, 72318-32-2; $\text{Fe}(\text{TPP})(\text{OCIO}_3)$, 57715-43-2.

Supplementary Material Available: Table II, atomic coordinates for $[\text{Fe}(\text{OEP})(3\text{-Clpy})_2](\text{ClO}_4)$, Table III, anisotropic thermal parameters, Table IV, rigid group parameters and derived atomic coordinates for the axial 3-chloropyridine ligands, Table VIII, a listing of the final refined hydrogen atom positions and listings of observed and calculated structure amplitudes ($\times 10$) for $[\text{Fe}(\text{OEP})(3\text{-Clpy})_2](\text{ClO}_4)$ at 98 and 293 K (77 pages). Ordering information is given on any current masthead page.

(41) Kirner, J. F.; Garofalo, J., Jr.; Scheidt, W. R. *Inorg. Nucl. Chem. Lett.* **1975**, *11*, 107–112.

(42) Sinn, E.; Sim, P. G.; Dose, E. V.; Tweedle, M. F.; Wilson, L. J. *J. Am. Chem. Soc.* **1978**, *100*, 3375–3390.

(43) Ewald, A. H.; Martin, R. L.; Sinn, E.; White, A. H. *Inorg. Chem.* **1969**, *9*, 1837–1846.

(44) Cukauskas, E. J.; Deaver, B. S., Jr.; Sinn, E. *J. Chem. Phys.* **1977**, *67*, 1257–1266, and references therein.

(45) Leipoldt, J. G.; Coppens, P. *Inorg. Chem.* **1973**, *12*, 2269–2274.

(46) An interesting question is whether there is a change in position of the iron in derivatives having nonequivalent axial ligands during the spin-state transition.

(39) Kirner, J. F.; Scheidt, W. R. *Inorg. Chem.* **1975**, *14*, 2081–2086.
(40) Scheidt, W. R.; Brinegar, A. C.; Kirner, J. F.; Reed, C. A. *Inorg. Chem.* **1979**, *18*, 3610–3612.